Russian Journal of Earth Sciences

On the Estimation of the Interannual Variability of the Ocean Surface Temperature in the Area of the Peruvian Upwelling

J. Martina*[,1], S. M. Gordeeva[1], and V. N. Malinin[1]

[1] Russian State Hydrometeorological University, St. Petersburg, Russia
* **Correspondence to:** Jimmy Martina, jimmyjmv1@hotmail.com.

Abstract: The interannual variability of the ocean surface temperature in the area of the Peruvian upwelling for the period 1980–2022 is considered according to the satellite archive GODAS (Global Ocean Data Assimilation System) using the methods of multivariate statistical analysis. Local foci of significant trends, for average annual Sea Surface Temperature (SST) values, were identified near the Peruvian offshore. Four regions (clusters) were obtained, which describe the variability of SST in front off Peru, which could be used to pretend to develop a prognostic oceanographic model. Furthermore, coincidences of temperature fluctuations were found between the first cluster and the region N3+4.

Keywords: Peruvian upwelling, ocean surface temperature, interannual variability, multivariate statistical analysis.

Citation: Martina, J., S. M. Gordeeva, and V. N. Malinin (2024), On the Estimation of the Interannual Variability of the Ocean Surface Temperature in the Area of the Peruvian Upwelling, *Russian Journal of Earth Sciences*, 24, ES2009, EDN: QUZFII, https://doi.org/10.2205/2024es000876

Introduction

It is known that the ocean and the atmosphere are a single interconnected system. Large-scale processes in this system have a decisive influence on the formation of weather and climate in South America, mainly in Peru [*Brink et al.*, 1983; *Karstensen and Ulloa*, 2009].

The Peruvian upwelling (PU) is driven by the interaction of oceanic and atmospheric factors and is one of the four highly productive upwelling areas in the oceans and the largest one in terms of fish catches [*Bakun and Weeks*, 2008; *Gutiérrez et al.*, 2016; *Heileman et al.*, 2009]. The PU is formed by the cold Peruvian Current, which comes from southern Chile and flows northward the equator. As a result of the wind blowing in the direction of the equator, the Coriolis force in the trade wind deflects the current to the west [*Karstensen and Ulloa*, 2009; *Ramos et al.*, 2022].

Upwelling process (the rise to the surface of high-nutrient water) contributes to the formation of important biological productivity of the area. In the waters of the Peruvian upwelling, it is about 0.02% of the area of the oceans, where almost 20% of the world's fish catch is produced [*Agüero and Claveri*, 2007; *Bakun*, 1996; *Bakun and Weeks*, 2008; *Bakun et al.*, 2010, 2015; *Bertrand et al.*, 2004; *Brink et al.*, 1983; *Castillo et al.*, 2018; *Chavez et al.*, 2008; *Espinoza-Morriberón et al.*, 2017; *FAO*, 2022; *Nixon and Thomas*, 2001].

Figure 1 shows the distribution in million tons of fish catches of the 10 largest fish-producing countries according to FAO data [*FAO*, 2022]. It is easy to see that their total catch reaches 57% of the world fishing. At the same time, the largest fishing country is China, which is twice ahead of Indonesia that is in the second place. It is China and Peru that get the most fish in the Peruvian Upwelling region.

For Peruvians, fishing is of great economic importance. Therefore, studying factors on bioproductivity in this region is not only important for scientific knowledge, but also practical. Therefore, the purpose of this article is to study the variability of sea water temperature because it has an important impact on the vital activity of marine organisms. Temperature changes can manifest itself in an explicit and indirect form since it can

Research Article

Received: 1 July 2023
Accepted: 16 October 2023
Published: 27 May 2024

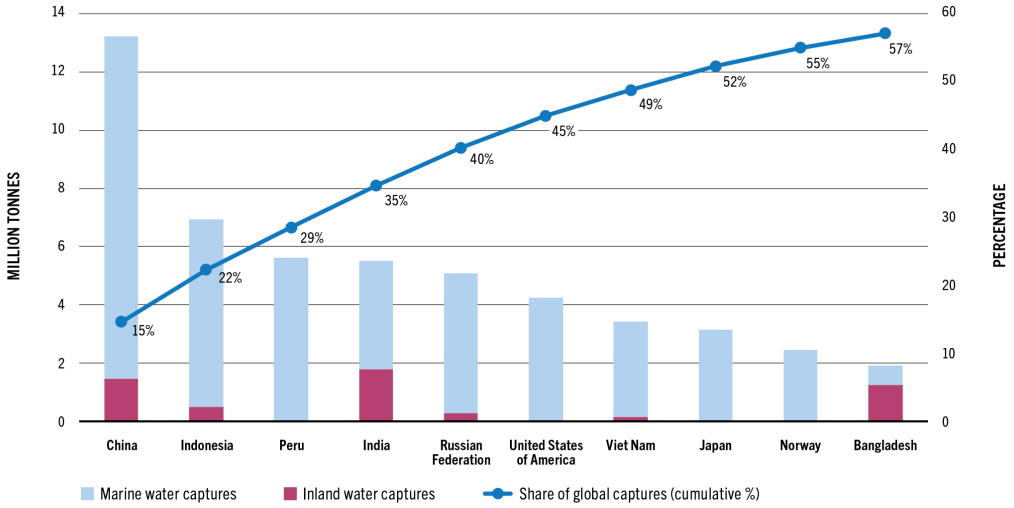

Figure 1. Distribution in million tons of fish catches of the 10 largest fish-producing countries in 2020 according to FAO data [*FAO*, 2022].

accelerate or slow down growth, and even lead to mass death during sudden temperature changes [*Bohle-Carbonell*, 1989; *Malinin*, 2002; *Penven et al.*, 2005; *Ramos et al.*, 2022; *Zavala et al.*, 2019].

With regard to modelling work off the coast of Peru, there were several publications in which oceanographic variables were considered as interconnected with each other. For example, [*Tarazona and Arntz*, 2001] proposed a joint model of satellite data on sea surface temperature (SST) and tidal sea level anomalies to study their interannual and interdecadal variability. [*Penven et al.*, 2005] and [*Aguirre*, 2015] were constantly working on modelling upwelling characteristics in different seasons of the year. In addition, [*Huaringa*, 2020; *Wang et al.*, 2019] modelled the wind and its effect on the surface waters of the sea.

[*Bakun*, 1996; *Bakun and Weeks*, 2008; *Bakun et al.*, 2010, 2015; *Bertrand et al.*, 2004] hypothesized that an increase in greenhouse gases will result in considerable changes in land-sea pressure gradients, which would affect global wind patterns and in the natural state, would eventually increase the upwelling pressure in the oceans. Then, in the case of developing a predictive ocean temperature model, it would be possible to determine fish landings to a certain extent [*Castillo et al.*, 2021; *Massing et al.*, 2022; *Penven et al.*, 2005; *Ramos et al.*, 2022; *Swartzman et al.*, 2008; *Zavala et al.*, 2019].

It was also said that there was no clear evidence of associated changes in wind dynamics [*Abrahams et al.*, 2021].

On the other hand, according to recent modelling [*Chang et al.*, 2023], upwelling systems in the Southern Hemisphere showed a future strengthening of coastal winds with rapid coastal warming, which cannot be explained by the Bakun hypothesis.

In addition, [*Krasnoborodko*, 2018] described the relationship between the displacement of the pole of the Earth's rotation axis relative to its geographic pole and fishing in the Peruvian subzone of the southeastern Pacific Ocean.

As a result, such processes would take part in the uncertainty on the construction of a predictive model.

The main goal of this work is to statistically analyze the interannual variability of SST in the Peruvian upwelling area, which includes a description of linear trends, zoning of the PU water area according to annual SST values using the methods of factor and cluster analysis, identification of cluster centres and their statistical analysis with an assessment of the relationship with the El Nino indices (ENSO).

Materials and Methods

For this purpose, the GODAS (Global Ocean Data Assimilation System) database was used. The GODAS system is based on the quasi-global configuration of the GFDL MOM.v3 (Geophysical Fluid Dynamics Laboratory Modular Ocean Model). The model area extends from 75°S up to 65°N and has a resolution of 1°×1° magnified to 1/3° north-south within 10° of the equator. The PU area is accepted within the boundaries from 4°S up to 40°S [*Tarazona and Arntz*, 2001] (Figure 2). A total 216 points of the grid area were identified, for which the average monthly values of SST for the period 1980–2020 were selected from the GODAS database. We consider a spatial resolution of 1°×1° optimal for studying large-scale SST variability.

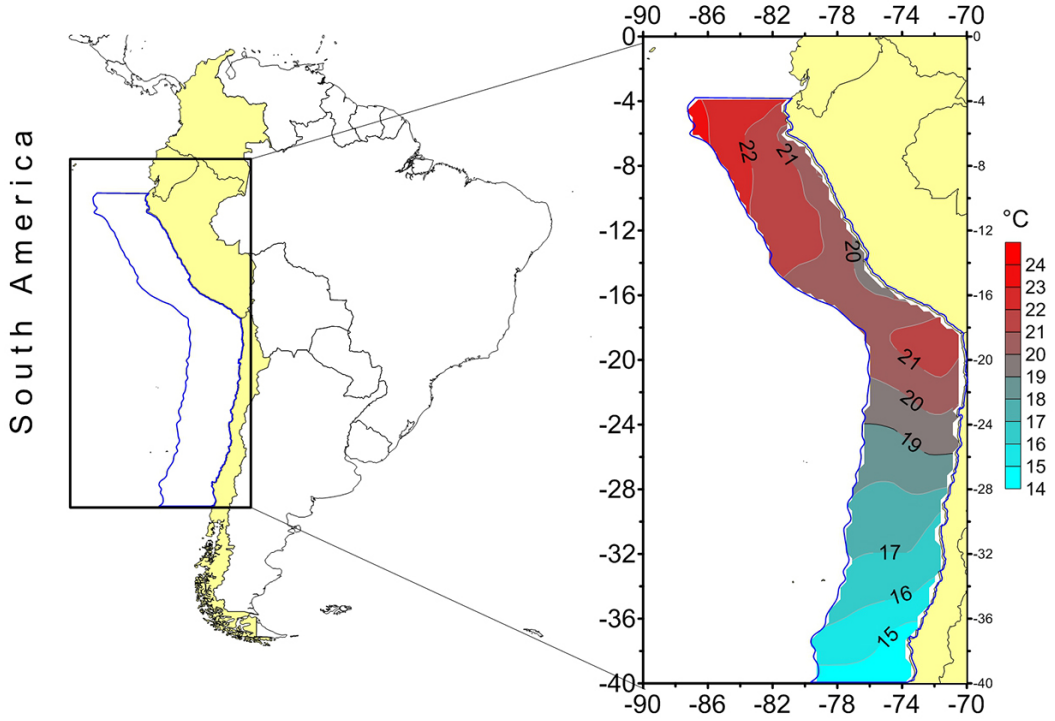

Figure 2. Selected region of the Peruvian upwelling (PU) and distribution of annual mean SST values for the period 1980–2020, computed from the GODAS database [http://apdrc.soest.hawaii.edu/dods/public_data/Reanalysis_Data/GODAS/monthly/].

Initially, statistical characteristics of annual SST values (arithmetic mean, standard deviation, trend value and its coefficient of determination) were calculated at grid nodes. The coefficient of determination was used to determine the contribution of the trend to the dispersion of the original series. The significance of the trend was assessed using the Student's t test at a p level of less than 0.05 [*Malinin*, 2002]. Multivariate statistical analysis methods were used to study the spatiotemporal variability and zonation of the SST field. Using the method of principal factors (PCA), it was possible to dramatically compress the information and move from a 216×41 matrix to a 216×4 matrix, i.e., to identify 4 quasi-homogeneous regions (clusters) in the interannual SST variability. The use of k-means cluster analysis method made it possible to optimally draw boundaries between regions. For each cluster, statistical centres were identified that best characterize large-scale SST variability within the cluster.

All analyses were performed using R Statistical Software (v4.1.2; R Core Team 2021) [*R Core Team*, 2021].

Results and Discussion

On the Spatial Distribution for the Average Annual SST Values

Figure 3 shows the spatial distribution of trend coefficients for annual mean SST values. From Figure 3 it is clear that negative SST trends are observed throughout the entire water area of the PU. Their maximum values (numbers in absolute value) are concentrated in a narrow coastal strip of the ocean in the northern part of PU between 6° and 16°S.

It can also be noted that for almost the entire PU region, with the exception of local hotspots in the north and south of PU, SST trends are significant. The reason for the negative trends in SST is the cold Peru Current, which is formed from the northern branch of the Antarctic Circumpolar Current.

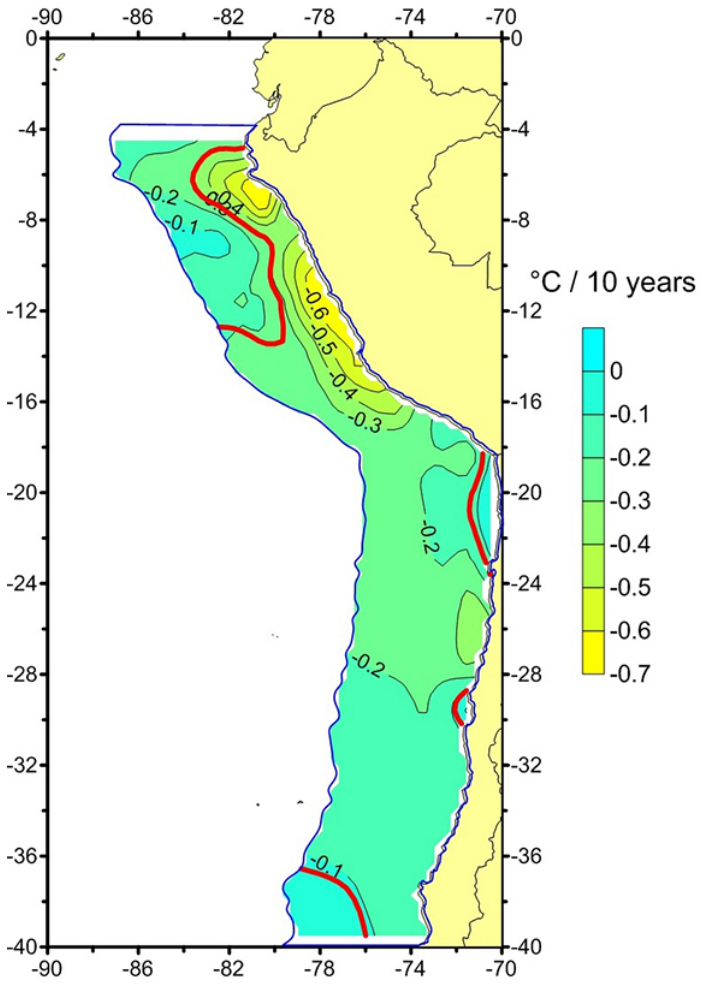

Figure 3. Spatial distribution of trend coefficients for average annual SST values in the Peruvian upwelling area. The thick red curve separates the local foci of insignificant trends.

At first glance, the relative cooling of the PU waters contradicts the well-known fact of the warming of the ocean waters. However, ocean warming is uneven. Although there is a well-defined increase in SST in most of the ocean, there are areas with negative trends. According to the Copernicus system [*ECMWF*, 2021], for the period 1993–2021, in the PU region and adjacent areas of the southeastern Pacific, a decrease in SST is observed, which is due to the cold Peruvian Current. It is also confirmed by [*Aiken et al.*, 2011], whose results showed that the alongshore wind increase off Peru and Chile led to a year-round upwelling intensification, then nearshore SST decrease.

In work [*Jebri et al.*, 2017] mentioned a conceptual hypothesis that the winds, that favour coastal upwelling, intensify with anthropogenic global warming. In fact, this hypothesis was examined by such authors for the dynamics of the Peru-Chile upwelling, covering the entire period of 1940-2014. They found evidence for intensification of upwelling-favourable winds in such a region. Furthermore, there are also evidences of wind-driven upwelling intensification continuously for 34 years (from 1980 to 2014) [*Jebri et al.*, 2020]. It is happening off Chile since the 1980s [*Falvey and Garreaud*, 2009] and off central-south Peru since the 1950s [*Abrahams et al.*, 2021; *Gutiérrez et al.*, 2011]. Other eastern boundary upwelling systems (EBUS) of the Southern Hemisphere such as the Benguela system off southern Africa [e.g., *Lamont et al.*, 2018] and the one west of Australia [e.g., *Rousseaux et al.*, 2012] do not appear to show any cooling.

Although there are different views on the reasons for the cooling, it would be triggered by the intensification of the zonal circulation of the atmosphere [*Malinin and Vainovsky*, 2020], the main parameter of which is the Southern Annular Mode (SAM), calculated directly from data on atmospheric pressure at meteorological stations between 40° and 65°S. Due to the intensification of the SAM, the Antarctic Circumpolar Current strengthens, including its northern branch, which forms the cold Peruvian Current. Evidence of the strengthening of the Peruvian Current is positive trends in sea level along the coast of South America [*Malinin and Smirnov*, 2022]. As a result, the vast water area in the PA zone is getting colder.

Spatiotemporal Variability and Zonation of the SST Field

In order to reveal the spatiotemporal connection of interannual variability of the SST field, the method of principal factors was used, the first stage of which is the method of

Table 1. Estimates of eigenvalues and the rate of their convergence of average annual SST values for 1980–2020, obtained by the method of principal factors

	First rotation			Second rotation		
λ_j	λ_j	λ_j/λ_j %	k_{rc}, %	λ_j	λ_j/λ_j %	k_{rc}, %
1	152.8	70.7	70.7	80.4	37.2	37.2
2	31.2	14.4	85.2	76.23	35.3	72.5
3	9.5	4.4	89.6	18.4	8.6	81.1
4	7.0	3.2	92.9	25.6	11.8	92.9

Note: λ_j – Eigenvalue, k_{rc} – Rate of convergence

principal components (PCA). A matrix of average annual SST values sized 216 × 41 was subjected to decomposition. A very high rate of convergence (k_{rc}) of the eigenvalues λ_j was found. Thus, already 1 eigenvalue λ_1 described more than 70% of the total dispersion of the SST field. In total, the first four λ_j described 93% of the dispersion of the SST field (Table 1). Analysis of the field values of the first expansion eigenvector showed that significant correlation coefficients cover the predominant part of the PU water area, i.e., the SST field looks homogeneous.

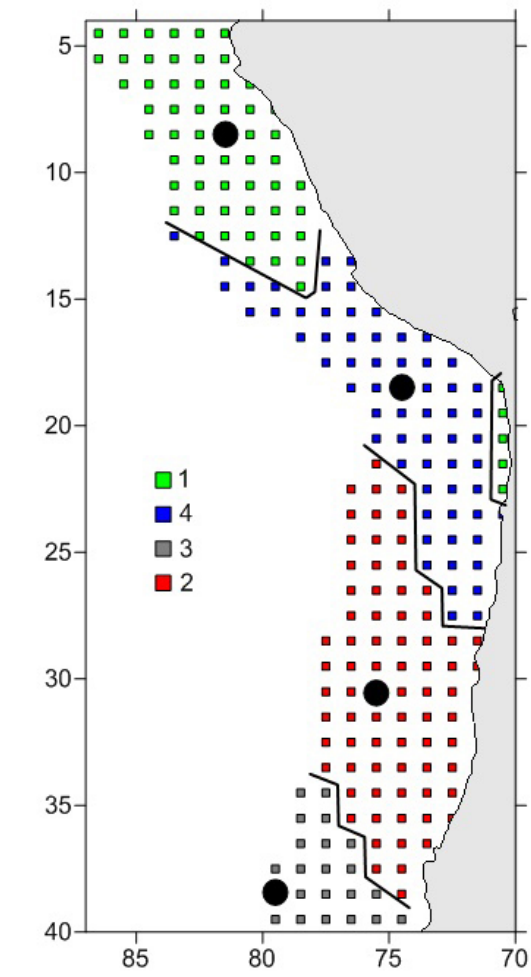

Figure 4. Results of zoning of the PU area according to the nature of interannual variability of SST. The numbers correspond to the factor numbers. Black dots indicate the centres of quasi-homogeneous regions, which optimally describe the variability of SST within the region.

Taking into account the large spatial extent of the PU region, such a result seemed unobvious. Therefore, the decomposition eigenvectors and the principal components of these 4 λ_j were subjected to a second rotation by Kaiser's varimax method. As a result of this rotation, the variance was transferred from the 1st common factor to the rest, and the 2nd factor increased by more than twice. Analysis of principal factors showed that more than 80% of the PU water area is described by the first three factor loadings (FL), which have estimates of more than 0.70. In the rest of the water area, FL estimates are "smeared out" relatively evenly, i.e., they are less than 0.65. The estimates of the fourth FL at all points of the PU water area turned out to be less than 0.65, i.e., it practically does not participate in the formation of the variability of the SST field.

According to the spatial distribution of FL values of more than 0.70, four territorially connected quasi-homogeneous regions are quite clearly distinguished in the PU water area. At the same time, four areas mainly include points with FL estimates less than 0.65. Note that, in this case, there is some uncertainty in drawing the boundaries between the regions. Finding the exact boundaries can be done using the k-means cluster analysis method, which minimizes the sum of squared intracluster distances to the cluster centre [*Malinin et al.*, 2002]. Distances between points were found using the traditional Euclidean metric. In Figure 4 the results of zoning of the PU area, according to the nature of the interannual variability of SST, are shown.

The highest FL is noted for region 1 (cluster 1) highlighted in Figure 4 in green. It included 59 points, which were located at the extreme northern position in the PU region. The centre of this cluster has coordinates 8.5°S. and 81.5°W, and its value (0.97) was the maximum for

the entire FL matrix. The second FL mainly forms the 2nd cluster (red color), which partially occupied the central and southern parts of the PU region, consists of 74 points, and the centre of the cluster has a value of 0.95. The smallest cluster 3 (22 points) was located in the extreme south of the PU.

Finally, cluster 4 is formed from FL values, mostly less than 0.65, and occupied an intermediate position between clusters 1 and 2. So, as a result of using the method of main factors, it was possible to reduce the dimension of the initial SST field to 4 points, which, in fact, describe the interannual variability of the SST field in the PU area.

Table 2 shows the statistical characteristics of the annual SST values in the cluster centres and the correlation coefficients between them; Figure 5 gives the interannual variation of SST in the centres of each cluster. It is easy to see that SST consistently decreases towards the south. The maximum amplitude is typical for region 1 (cluster 1). During El Niño, there was a sharp increase in SST. In the interannual course of the SST, for each of these clusters, a negative trend was manifested, which was most pronounced in the SST for cluster 4. For clusters 1 and 3, the trend was insignificant. As for the correlation of annual SST values in the centres of clusters, it varied from 0.67 between clusters 1 and 4 to 0.30 between extreme clusters 1 and 3.

Table 2. Statistical characteristics of annual SST values in cluster centres and correlation coefficients between them

Cluster	X_{av}, °C	A, °C	C	Tr, °C/10 years	R^2	Correlation		
						2	3	4
1	21.6	4.9	0.05	−0.17	0.04	0.41	0.30	0.67
2	17.3	1.6	0.02	−0.13	0.18	1	0.43	0.65
3	15.2	1.5	0.02	−0.04	0.02		1	0.46
4	20.8	2.7	0.03	−0.26	0.32			1

Note: X_{av} – average, A – amplitude, C – coefficient of variation, Tr – trend coefficient, R^2 – trend determination coefficient

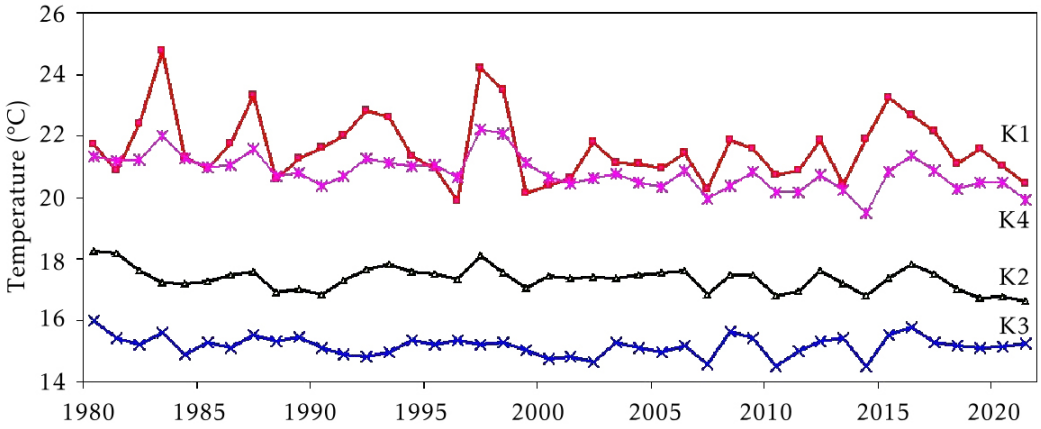

Figure 5. Interannual variation of SST in the centres of each cluster.

On the Peruvian Upwelling System and ENSO Region

The El Niño-Southern Oscillation region (ENSO) is a unique hydrometeorological phenomenon. It is the largest and most powerful energy-active zone of the World Ocean, which has an extremely important influence on the formation of long-term weather fluctuations and short-term climate fluctuations not only in the Pacific Ocean, but also far beyond its borders. At the same time, ENSO is the most powerful source of CO_2 flow from the ocean to the atmosphere, which is characterized by a significant positive trend [*Malinin and*

Vainovsky, 2022]. Given the proximity of ENSO to PU, it is natural to expect a relationship between them. More than a dozen different ENSO indices are known, but the central place among them is occupied by the Nino 3.4 region (5°N–5°S, 120°W–170°W), which is most closely related to other indices and is most often used in research.

What is also important for us is the N1+2 region (0°–10°S and 80°W–90°W), which is located in the northern and central part of the Peruvian Sea and is partially included in the PU zone, which is under consideration in this research. It is influenced by the strong Equatorial Undercurrent (EUC), which reaches the Peruvian shelf [*Rosales Quintana et al.*, 2021] and most clearly determines the occurrence and extent of the El Niño event in coastal Peru [*SENAMHI*, 2014].

Figure 6 shows the interannual variation of annual SST values in areas N3.4, N1+2 and in the centre of the first cluster of Peruvian upwelling. It is easy to see that there is a high degree of identity between these variables: positive (El Niño phenomenon) and negative (La Niña phenomenon) SST practically coincide. However, the strength of the relationship between the variables varies markedly. Naturally, the connection between the SST in the N1+2 region and the centre of cluster 1 is almost functional ($r = 0.92$). The connection between SST in the region N3.4 and the centre of cluster 1 is noticeably lower ($r = 0.70$). Note that the connection between SST in N3+4 and SST in more southern clusters sharply decreases and becomes insignificant for clusters 2 and 3. Thus, the influence of ENSO, as expected, extends predominantly to the northern PU zone.

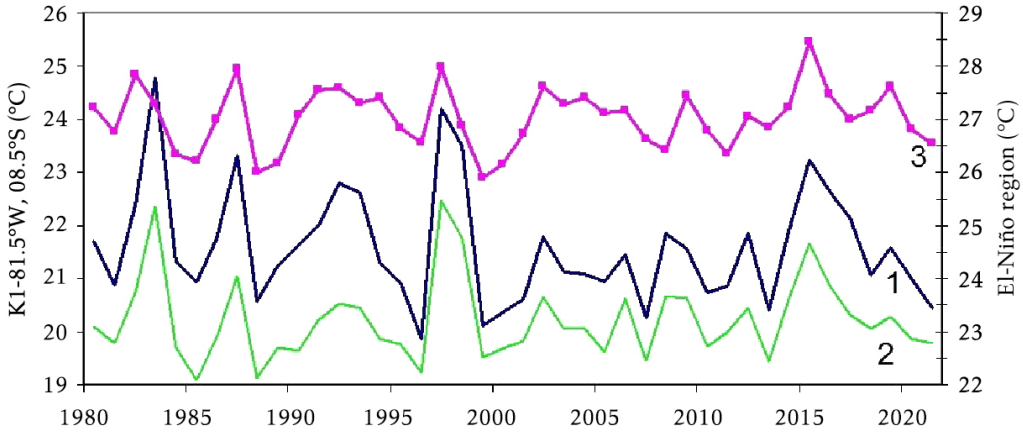

Figure 6. Interannual variation of SST in the centre of cluster 1 of PU (1), at the regions N1+2 (2) and N3.4 (3).

Conclusions

It is shown that the PU water area is characterized by negative trends in annual SST values for the period 1980–2020, imported from the GODAS (Global Ocean Data Assimilation System) system. Although there are different views on the reasons for the cooling, the most realistic, in our opinion, is the assumption that it is caused by the intensification of zonal atmospheric circulation, the main parameter of which is the Southern Annular Mode (SAM), calculated directly from data on atmospheric pressure at meteorological stations between 40° and 65°S. As a result of the intensification of the SAM, the Antarctic Circumpolar Current strengthens, including its northern branch, which forms the cold Peruvian Current. As a result, the vast water area in the PU zone is getting colder.

To zonate the SST field according to the nature of interannual fluctuations, the methods of principal factors and k-means cluster analysis were used. It is shown that the first four eigenvalues of the expansion of the original matrix of annual SST anomalies of size 216×41 describe almost 93% of the variance of the original SST field. As a result, it was possible to reduce the dimension of the SST field to 216×4. Then, the resulting matrix of factor loadings was subjected to clustering using the k-means method, which minimizes the

sum of the squares of intracluster distances to the cluster centre. This made it possible to obtain an optimal partition of the SST field (216 points) into 4 quasi-homogeneous areas territorially connected to each other. Naturally, cluster 1 included a larger number of points with the highest factors (0.70–0.97). In each cluster, a statistical centre was identified that optimally characterizes the interannual variability of the SST field within the cluster. Thus, the combined usage of the main factors method (PCA) and the k-means cluster analysis method made it possible to reduce the dimension of the original SST field to 4 points, which essentially describe the interannual variability of the SST field in the PU region.

The statistical characteristics of annual SST values in the centres of clusters and the correlation coefficients between them are considered. The highest amplitude of oscillations is characteristic of cluster 1. Southward, the amplitude of SST fluctuations decreases. A high degree of connection between the SST of the northern cluster and the ENSO indices (N3+4 and N1+2) is shown. There is a complete evident correspondence of SST to the El Niño and La Niña phenomena. As expected, the connection between SST in the N1+2 region and the centre of cluster 1 is almost functional ($r = 0.92$). The connection between SST in the N3.4 region and the centre of cluster 1 is noticeably lower ($r = 0.70$). For more southern clusters, the correlation decreases sharply and becomes insignificant for clusters 2 and 3.

Acknowledgements. The authors are grateful to the respected reviewers for the insightful comments and valuable improvements to our paper. Furthermore, we thank Anastasia Bondarenko for checking translation.

References

Abrahams, A., R. W. Schlegel, and A. J. Smit (2021), Variation and Change of Upwelling Dynamics Detected in the World's Eastern Boundary Upwelling Systems, *Frontiers in Marine Science*, *8*, https://doi.org/10.3389/fmars.2021.626411.

Aguirre, E. H. (2015), A Numerical Study of Oceanic Circulation in San Juan, Peru. Calibration of Princeton Ocean Model During 1991-2000, *The Open Oceanography Journal*, *8*(1), 33–38, https://doi.org/10.2174/1874252101408010033.

Agüero, M., and M. Claveri (2007), Capacidad de pesca y manejo pesquero en América Latina y el Caribe: Una síntesis de casos, in *Capacidad De Pesca Y Manejo Pesquero En America Y El Caribe (Documento Tecnicos De Pesca)*, vol. 461, pp. 61–71, Food & Agriculture Org.

Aiken, C. M., S. A. Navarrete, and J. L. Pelegrí (2011), Potential changes in larval dispersal and alongshore connectivity on the central Chilean coast due to an altered wind climate, *Journal of Geophysical Research*, *116*(G4), https://doi.org/10.1029/2011JG001731.

Bakun, A. (1996), *Patterns in the Ocean: Ocean Processes and Marine Population Dynamics*, 346 pp., California Sea Grant, San Diego (CA).

Bakun, A., and S. J. Weeks (2008), The marine ecosystem off Peru: What are the secrets of its fishery productivity and what might its future hold?, *Progress in Oceanography*, *79*(2–4), 290–299, https://doi.org/10.1016/j.pocean.2008.10.027.

Bakun, A., D. B. Field, A. Redondo-Rodriguez, and S. J. Weeks (2010), Greenhouse gas, upwelling-favorable winds, and the future of coastal ocean upwelling ecosystems, *Global Change Biology*, *16*(4), 1213–1228, https://doi.org/10.1111/j.1365-2486.2009.02094.x.

Bakun, A., B. A. Black, S. J. Bograd, M. García-Reyes, A. J. Miller, R. R. Rykaczewski, and W. J. Sydeman (2015), Anticipated Effects of Climate Change on Coastal Upwelling Ecosystems, *Current Climate Change Reports*, *1*(2), 85–93, https://doi.org/10.1007/s40641-015-0008-4.

Bertrand, A., M. Segura, M. Gutiérrez, and L. Vásquez (2004), From small-scale habitat loopholes to decadal cycles: a habitat-based hypothesis explaining fluctuation in pelagic fish populations off Peru, *Fish and Fisheries*, *5*(4), 296–316, https://doi.org/10.1111/j.1467-2679.2004.00165.x.

Bohle-Carbonell, M. (1989), On the variability of the Peruvian upwelling system, in *The Peruvian upwelling ecosystem: dynamics and interactions*, pp. 14–32, ICLARM Conference Proceedings Instituto del Mar del Perá (IMARPE).

Brink, K. H., D. Halpern, A. Huyer, and R. L. Smith (1983), The physical environment of the Peruvian upwelling system, *Progress in Oceanography*, *12*(3), 285–305, https://doi.org/10.1016/0079-6611(83)90011-3.

Castillo, R., L. Dalla Rosa, W. García Diaz, L. Madureira, M. Gutierrez, L. Vásquez, and R. Koppelmann (2018), Anchovy distribution off Peru in relation to abiotic parameters: A 32-year time series from 1985 to 2017, *Fisheries Oceanography*, *28*(4), 389–401, https://doi.org/10.1111/fog.12419.

Castillo, R., R. Cornejo, L. La Cruz, D. Grados, G. Cuadros, A. Paz, and M. Pozada (2021), Abundancia de anchoveta (Engraulis ringens) y otras especies pelágicas estimadas por el método hidroacústico en el ecosistema marino peruano en el 2020, *Informe Instituto del Mar de Perú*.

Chang, P., G. Xu, J. Kurian, R. J. Small, G. Danabasoglu, S. Yeager, F. Castruccio, Q. Zhang, N. Rosenbloom, and P. Chapman (2023), Uncertain future of sustainable fisheries environment in eastern boundary upwelling zones under climate change, *Communications Earth & Environment*, *4*(1), https://doi.org/10.1038/s43247-023-00681-0.

Chavez, F. P., A. Bertrand, R. Guevara-Carrasco, P. Soler, and J. Csirke (2008), The northern Humboldt Current System: Brief history, present status and a view towards the future, *Progress in Oceanography*, *79*(2–4), 95–105, https://doi.org/10.1016/j.pocean.2008.10.012.

ECMWF (2021), Sea surface temperature: climate indicators, https://climate.copernicus.eu/climate-indicators/sea-surface-temperature, (date of access: 03.02.2023).

Espinoza-Morriberón, D., V. Echevin, F. Colas, J. Tam, J. Ledesma, L. Vásquez, and M. Graco (2017), Impacts of El Niño events on the Peruvian upwelling system productivity, *Journal of Geophysical Research: Oceans*, *122*(7), 5423–5444, https://doi.org/10.1002/2016JC012439.

Falvey, M., and R. D. Garreaud (2009), Regional cooling in a warming world: Recent temperature trends in the southeast Pacific and along the west coast of subtropical South America (1979-2006), *Journal of Geophysical Research: Atmospheres*, *114*(D4), https://doi.org/10.1029/2008JD010519.

FAO (2022), *State of World Fisheries and Aquaculture 2022. Towards Blue Transformation*, 266 pp., Food & Agriculture Organization of the United Nations, Rome, https://doi.org/10.4060/cc0461en.

Gutiérrez, D., I. Bouloubassi, A. Sifeddine, et al. (2011), Coastal cooling and increased productivity in the main upwelling zone off Peru since the mid-twentieth century: RECENT TRENDS IN THE PERUVIAN UPWELLING, *Geophysical Research Letters*, *38*(7), https://doi.org/10.1029/2010GL046324.

Gutiérrez, D., M. Akester, and L. Naranjo (2016), Productivity and Sustainable Management of the Humboldt Current Large Marine Ecosystem under climate change, *Environmental Development*, *17*, 126–144, https://doi.org/10.1016/j.envdev.2015.11.004.

Heileman, S., R. Guevara, F. Chavez, A. Bertrand, and H. Soldi (2009), XVII-56 Humboldt current: LME # 13, in *The UNEP Large marineEcosystem Report: A perspective on changing conditions in LMEs of the world's Regional Seas*, United Nations Environment Programme, Nairobi (Kenya).

Huaringa, E. (2020), The Peruvian upwelling system. A numerical study of the spatial and time variabilities, *Revista De Investigación De Física*, *23*(3), 31–36.

Jebri, B., M. Khodri, G. Gastineau, V. Echevin, and S. Thiria (2017), Intensification of Chile-Peru upwelling under climate change: diagnosing the impact of natural and anthropogenic forcing from the IPSL-CM5 model, in *AGU Fall Meeting Abstracts*, American Geophysical Union.

Jebri, B., M. Khodri, V. Echevin, G. Gastineau, S. Thiria, J. Vialard, and N. Lebas (2020), Contributions of Internal Variability and External Forcing to the Recent Trends in the Southeastern Pacific and Peru-Chile Upwelling System, *Journal of Climate*, *33*(24), 10,555–10,578, https://doi.org/10.1175/JCLI-D-19-0304.1.

Karstensen, J., and O. Ulloa (2009), Peru-Chile Current System, in *Encyclopedia of Ocean Sciences*, pp. 385–392, Elsevier, https://doi.org/10.1016/b978-012374473-9.00599-3.

Krasnoborodko, O. (2018), On recurrence of heavy and disastrous El Niño and its impact on fishery in the Peruvian subarea of the South-East Pacific, *Proceedings of AtlantNIRO*, *2*(2), 66–83 (in Russian).

Lamont, T., M. García-Reyes, S. J. Bograd, C. D. van der Lingen, and W. J. Sydeman (2018), Upwelling indices for comparative ecosystem studies: Variability in the Benguela Upwelling System, *Journal of Marine Systems*, *188*, 3–16, https://doi.org/10.1016/j.jmarsys.2017.05.007.

Malinin, V. (2002), *Statistical Methods for the Analysis of Hydrometeorological Information*, 408 pp., Russian State Hydrometeorological University (RSHU), St. Petersburg (in Russian).

Malinin, V., P. Chernyshkov, and S. Gordeeva (2002), *Canarian upwelling: Large-scale variability and forecast of water temperature*, 156 pp., Gidrometeoizdat (in Russian).

Malinin, V. N., and M. A. Smirnov (2022), Sea level variability in the ENSO region of the Pacific Ocean, *Hydrometeorology and Ecology. Proceedings of the Russian State Hydrometeorological University*, (68), 463–477, https://doi.org/10.33933/2713-3001-2022-68-463-477 (in Russian).

Malinin, V. N., and P. A. Vainovsky (2020), Interannual variability in sea ice area of the Antarctic regions, *Sovremennye problemy distantsionnogo zondirovaniya Zemli iz kosmosa*, *17*(3), 187–201, https://doi.org/10.21046/2070-7401-2020-17-3-187-201 (in Russian).

Malinin, V. N., and P. A. Vainovsky (2022), On the interannual variability of the most intense sources and sinks of CO2 in the ocean based on observational data, *Hydrometeorology and Ecology. Proceedings of the Russian State Hydrometeorological University*, (66), 51–70, https://doi.org/10.33933/2713-3001-2022-66-51-70 (in Russian).

Massing, J. C., A. Schukat, H. Auel, D. Auch, et al. (2022), Toward a Solution of the "Peruvian Puzzle": Pelagic Food-Web Structure and Trophic Interactions in the Northern Humboldt Current Upwelling System Off Peru, *Frontiers in Marine Science*, *8*, https://doi.org/10.3389/fmars.2021.759603.

Nixon, S., and A. Thomas (2001), On the size of the Peru upwelling ecosystem, *Deep Sea Research Part I: Oceanographic Research Papers*, *48*(11), 2521–2528, https://doi.org/10.1016/S0967-0637(01)00023-1.

Penven, P., V. Echevin, J. Pasapera, F. Colas, and J. Tam (2005), Average circulation, seasonal cycle, and mesoscale dynamics of the Peru Current System: A modeling approach, *Journal of Geophysical Research: Oceans*, *110*(C10), https://doi.org/10.1029/2005JC002945.

R Core Team (2021), The R Project for Statistical Computing, https://www.R-project.org/, (date of access: 03.02.2023).

Ramos, J. E., J. Tam, V. Aramayo, F. A. B. no, et al. (2022), Climate vulnerability assessment of key fishery resources in the Northern Humboldt Current System, *Scientific Reports*, *12*(1), https://doi.org/10.1038/s41598-022-08818-5.

Rosales Quintana, G. M., R. Marsh, and L. A. Icochea Salas (2021), Interannual variability in contributions of the Equatorial Undercurrent (EUC) to Peruvian upwelling source water, *Ocean Science*, *17*(5), 1385–1402, https://doi.org/10.5194/os-17-1385-2021.

Rousseaux, C. S. G., R. Lowe, M. Feng, A. M. Waite, and P. A. Thompson (2012), The role of the Leeuwin Current and mixed layer depth on the autumn phytoplankton bloom off Ningaloo Reef, Western Australia, *Continental Shelf Research*, *32*, 22–35, https://doi.org/10.1016/j.csr.2011.10.010.

SENAMHI (2014), El fenómeno EL NIÑO en el Perú, http://issuu.com/senamhi_peru/docs/el_nino.

Swartzman, G., A. Bertrand, M. Gutiérrez, S. Bertrand, and L. Vasquez (2008), The relationship of anchovy and sardine to water masses in the Peruvian Humboldt Current System from 1983 to 2005, *Progress in Oceanography*, *79*(2–4), 228–237, https://doi.org/10.1016/j.pocean.2008.10.021.

Tarazona, J., and W. Arntz (2001), The Peruvian Coastal Upwelling System, in *Coastal Marine Ecosystems of Latin America*, pp. 229–244, Springer Berlin Heidelberg, https://doi.org/10.1007/978-3-662-04482-7_17.

Wang, L., H. Gao, J. Shi, and L. Xie (2019), A Numerical Study on the Impact of High-Frequency Winds on the Peru Upwelling System during 2014-2016, *Journal of Marine Science and Engineering*, *7*(5), 161, https://doi.org/10.3390/jmse7050161.

Zavala, R., D. Gutiérrez, R. Morales, et al. (Eds.) (2019), *Avances del Perú en la adaptación al cambio climático del sector pesquero y del ecosistema marino-costero*, 125 pp., Banco Interamericano de Desarrollo, https://doi.org/10.18235/0001647.